

Supporting Information

Strengthening Oxygen Reduction Activity on the Cooperation of Pyridinic-N and Graphitic-N for Atomically Dispersed Fe Sites

Gengyu Xing, Guangying Zhang, Baoluo Wang, Miaomiao Tong, Chungui Tian, Lei Wang,*
Honggang Fu*

Key Laboratory of Functional Inorganic Material Chemistry Ministry of Education of the
People's Republic of China, Heilongjiang University, Harbin 150080, China.

E-mail: wanglei0525@hlju.edu.cn; fuhg@vip.sina.com; fuhg@hlju.edu.cn

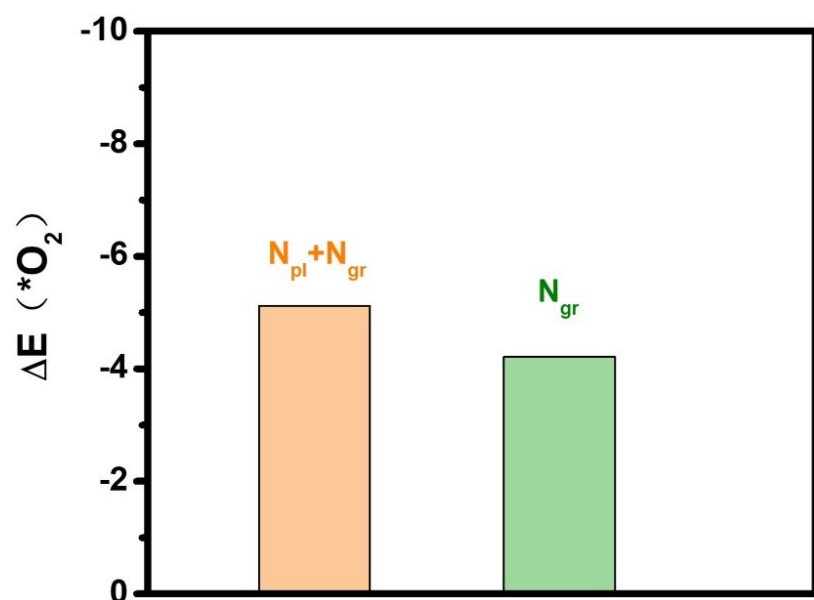


Fig. S1 Calculated O₂ adsorption energy for the N_{pl}+N_{gr} and N_{gr} models.

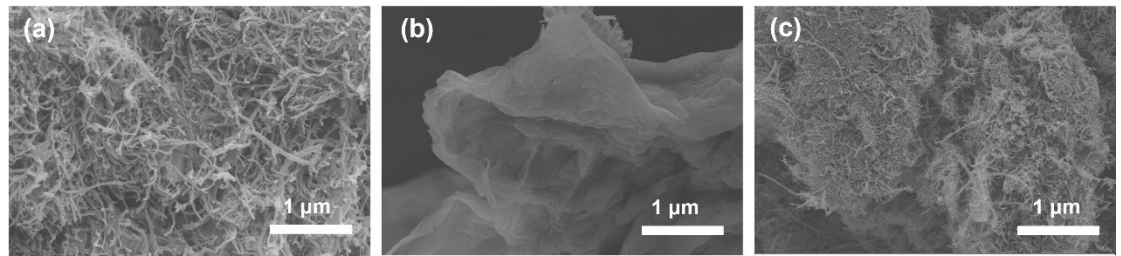


Fig. S2 SEM images of (a) Fe–N–C/CNT, (b) Fe–N–C/rGO, and (c) Fe–N–C/GC without freeze-drying.

Table S1. Mass contents of Fe in Fe–N–C/GC, Fe–FA–C/GC and Fe–Urea–C/GC sample tested by ICP-OES.

Samples	Mass content of Fe (wt.%)
Fe–N–C/GC	1.74
Fe–FA–C/GC	0.83
Fe–Urea–C/GC	0.51

Table S2. BET specific surface area values for all the compared samples.

Catalyst	BET surface area (m ² g ⁻¹)
Fe–N–C/GC	454.2
Fe–FA–C/GC	349.7
Fe–Urea–C/GC	171.2

Table S3. The contents of C, N, O and Fe for the prepared catalysts obtained from XPS spectra in Figure 3d.

	Atom Concentrations (%)				Mass Contents (%)			
	C	N	O	Fe	C	N	O	Fe
Fe–N–C/GC	83.72	5.28	10.52	0.47	76.19	5.60	18.21	0
Fe–FA–C/GC	91.41	1.34	7.25	0	89.07	1.52	9.41	0
Fe–Urea–C/GC	90.17	2.82	6.47	0.54	86.23	3.15	10.62	0

Table S4. The content of different N types for the prepared catalysts calculated from N 1s XPS in Figure 3f.

Sample	Pyridinic-N (%)	Pyrrolic-N (%)	Graphitic-N (%)
Fe–N–GC	59.82	11.11	29.07
Fe–FA–C/GC	50.60	33.91	15.49
Fe–Urea–C/GC	40.92	35.67	23.41

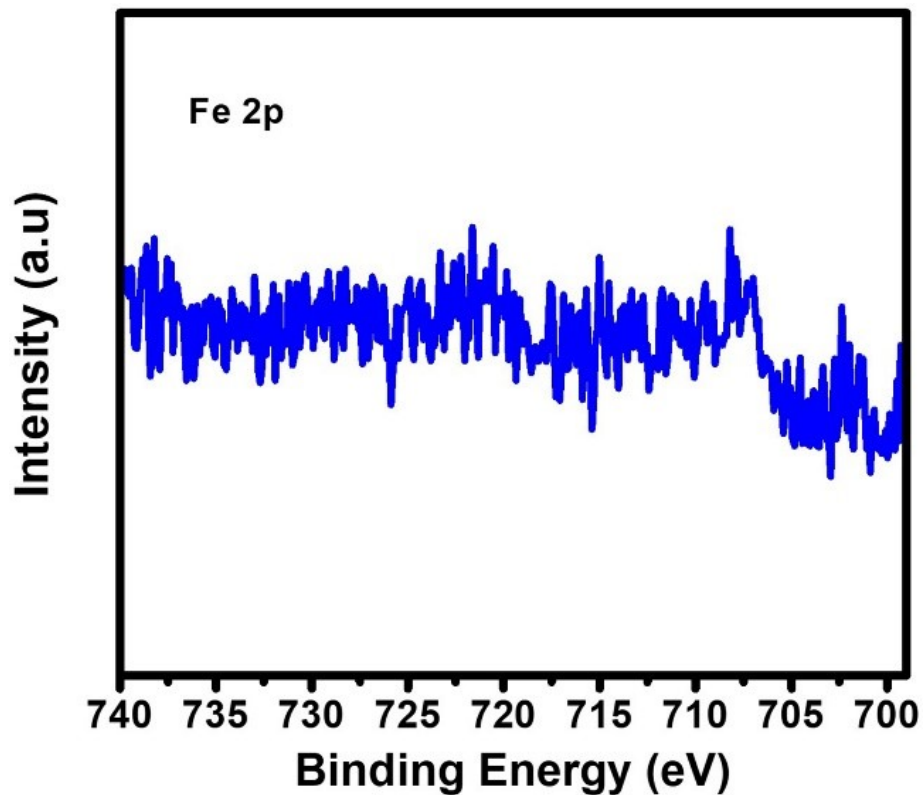


Fig. S3 High-resolution Fe 2p XPS spectrum of Fe–N–C/GC.

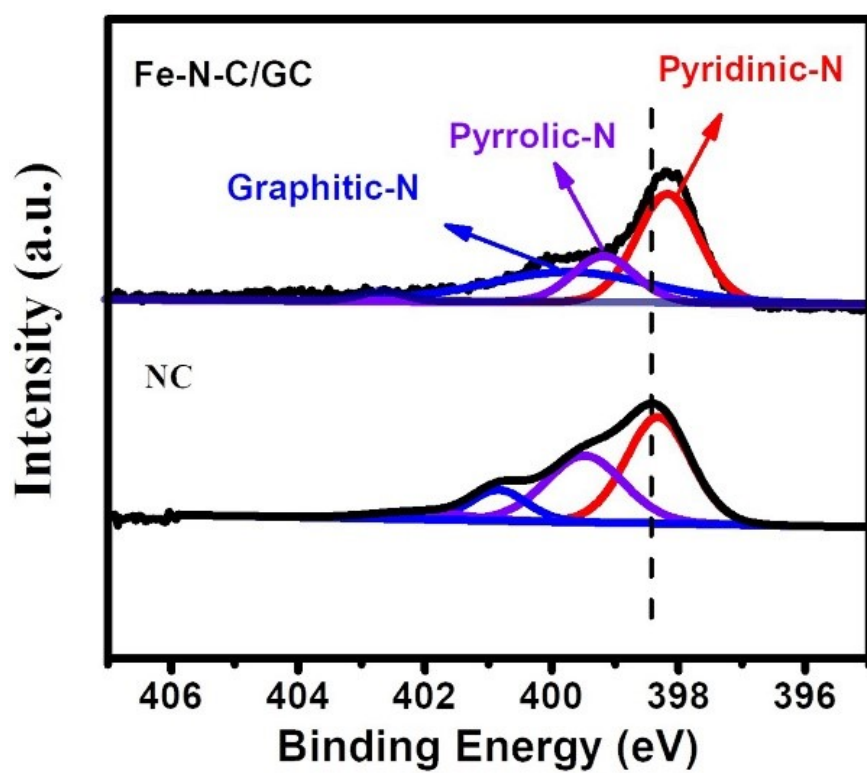


Fig. S4 High-resolution N 1s XPS spectra of Fe–N–C/GC and NC.

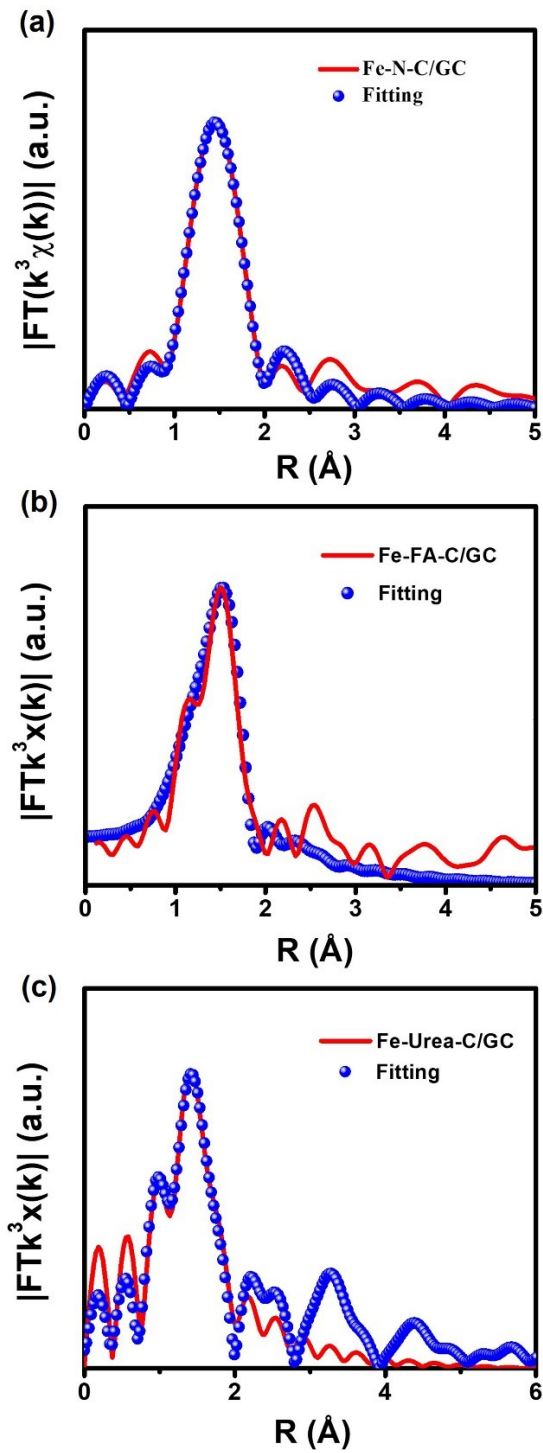


Fig. S5 FT-EXAFS fitting spectra of Fe K-edge for (a) Fe–N–C/GC, (b) Fe–FA–C/GC and (c) Fe–Urea–C/GC.

Table S5. FT-EXAFS fitting results from Figure 4.

Samples	Shell	N	ΔE_0 (e)	R(Å)	R-factor (%)
Fe–N–C/GC	Fe–N	4.100±0.2	–2.095	2.010±0.02	
Fe–FA–C/GC	Fe–N	3.729±0.2	–3.5534	1.999±0.02	<0.01
Fe–Urea–C/GC	Fe–N	4.73±0.1	0.48	2.010± 0.02	

Note: N: coordinated number; R: Bond distance; ΔE_0 , inner potential correction; All the R factors for the fitted results are within 0.02, indicating the goodness of the fitting.

Table S6. Comparison the ORR performances of Fe–N–C/GC with the reported nonprecious based SAS catalysts tested in 0.1 M KOH media.

Catalysts	$E_{1/2}$ (V vs. RHE)	References
Fe–N–C/GC	0.86	This work
FeHis-700	0.85	Small, 2016, 12, 5414-5421
Fe@C-NG/NCNTs	0.84	J. Mater. Chem. A, 2018, 6, 516-526.
Fe ₃ C/Fe@G-800	0.80	ACS Sustain. Chem. Eng., 2018, 6, 4890-4898.
SA-Fe-HPC	0.85	Angew. Chem., Int. Ed., 2018, 57, 9038-9043.
Fe ₃ -NG	0.86	Adv. Funct. Mater., 2016, 26, 5708-5717.
SA-Fe-NHPC	0.85	Adv. Mater. 2020, 32, 1907399
FeNx-PNC	0.84	ACS Nano, 2018, 12, 1949-1958
NCAG/Fe–Fe	0.85	Angew. Chem., Int. Ed. 2022, 61, e202201007
GO-Fe–N	0.82	ACS Catal. 2022, 12, 1601–1613

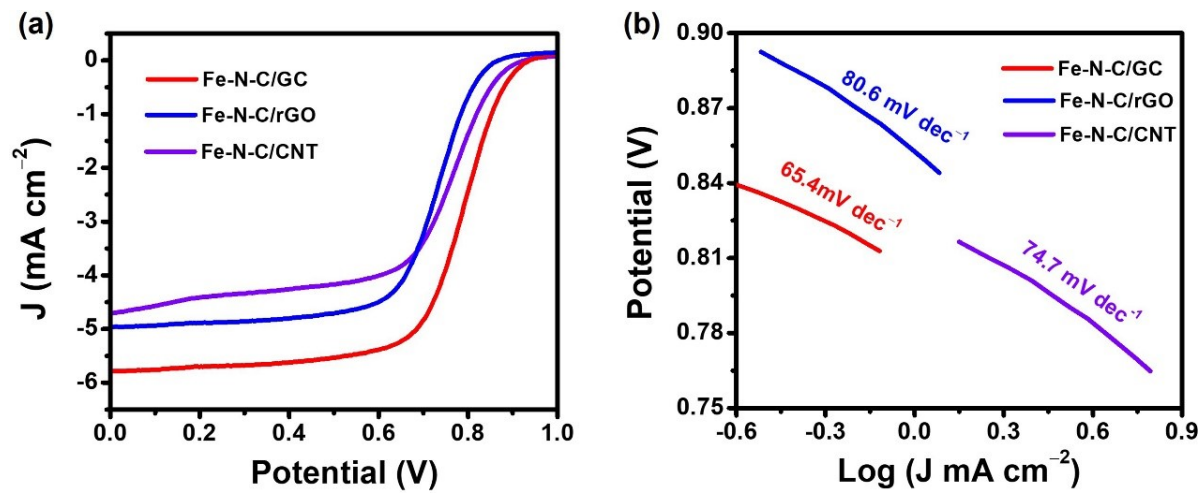


Fig. S6 (a) LSV curves and (b) the corresponding Tafel curves of Fe–N–C/CNT, Fe–N–C/rGO, Fe–N–C/GC tested in O_2 –saturated 0.1 M KOH electrolyte with a scanning rate of 5 mVs^{-1} at 1600 rpm.

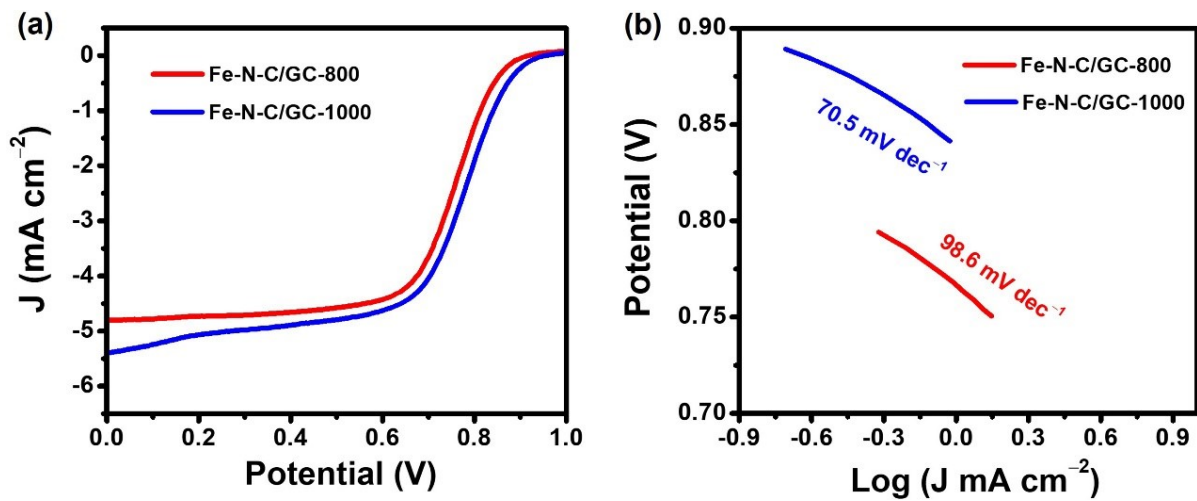


Fig. S7 (a) LSV curves and (b) the corresponding Tafel curves of Fe–N–C/GC-800 and Fe–N–C/GC-1000 tested in O₂–saturated 0.1 M KOH electrolyte with a scanning rate of 5 mV s⁻¹ at 1600 rpm.

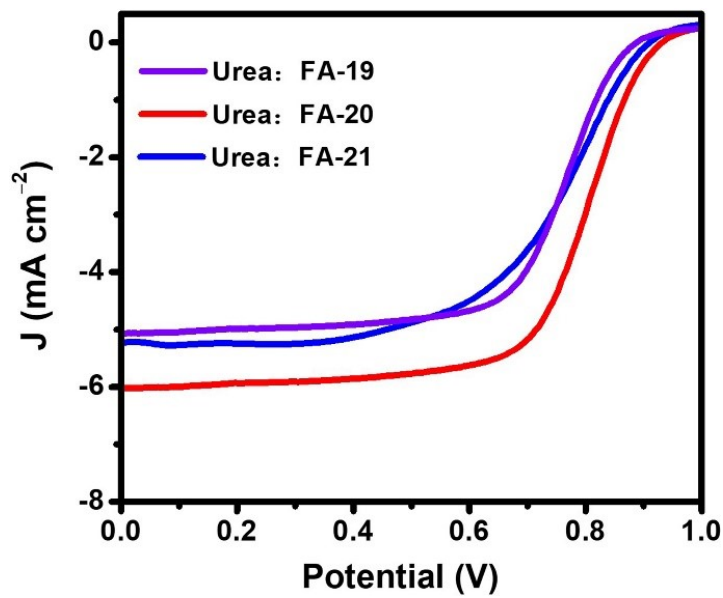


Fig. S8 (a) LSV curves of Urea:FA-19, Urea:FA-20 and Urea:FA-21 tested in O_2 -saturated 0.1 M KOH electrolyte with a scanning rate of 5 mV s^{-1} at 1600 rpm.

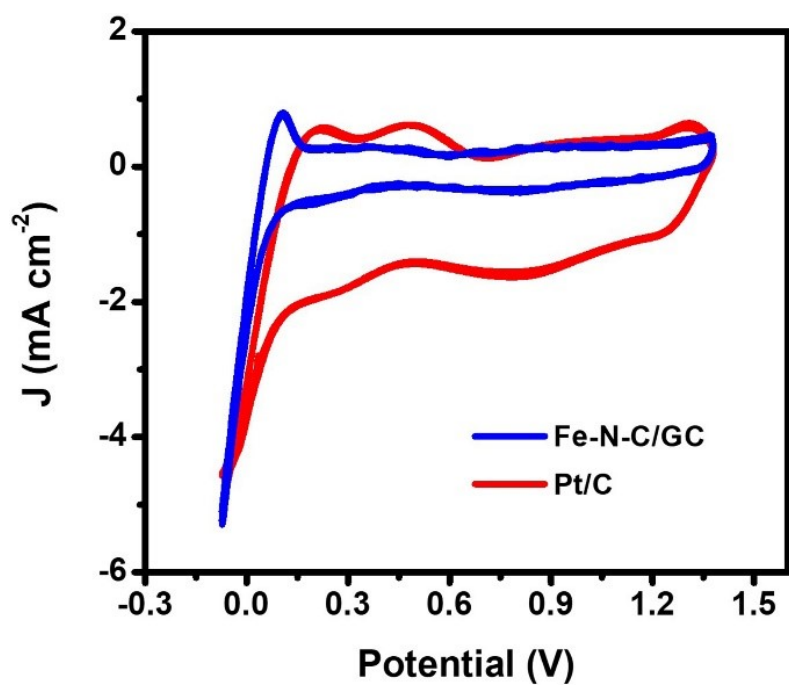


Fig. S9 (a) CV curves of Fe–N–C/GC and Pt/C tested in O₂–saturated 0.1 M KOH electrolyte at a scanning rate of 5 mV s^{−1}.

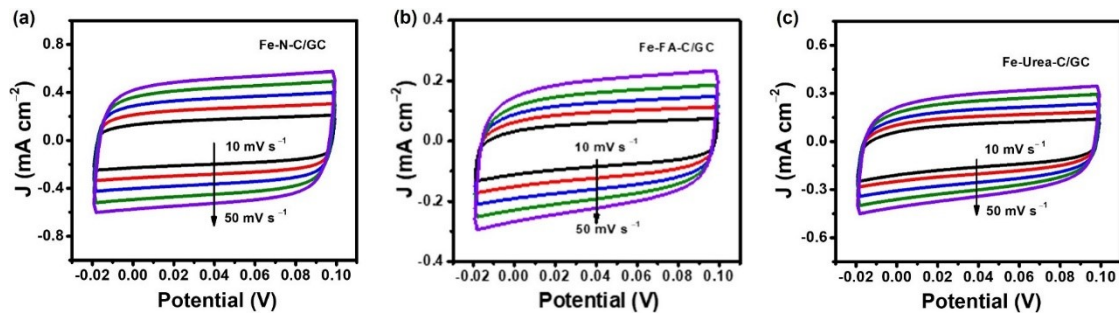


Fig. S10 CV curves of (a) Fe–N–C/GC, (b) Fe–FA–C/GC and (c) Fe–Urea–C/GC tested in O_2 –saturated 0.1 M KOH electrolyte at the scan rates of 5, 10, 15, 20 and 25 $mV s^{-1}$.

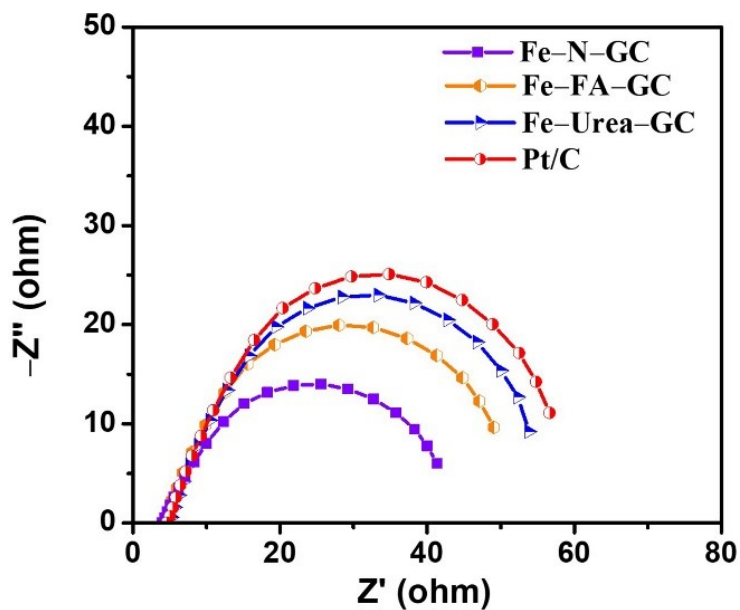


Fig. S11 EIS Nyquist plots for Fe–N–C/GC, Fe–FA–C/GC, Fe–Urea–C/GC and Pt/C.

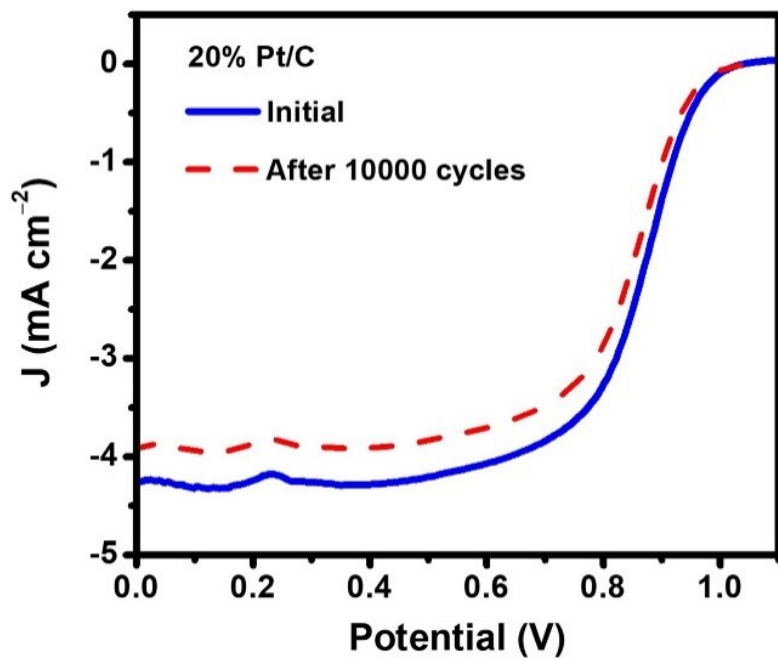


Fig. S12 LSV curves of Pt/C at 1600 rpm with a scan rate of 5 mV s^{-1} before and after 10000 cycles.

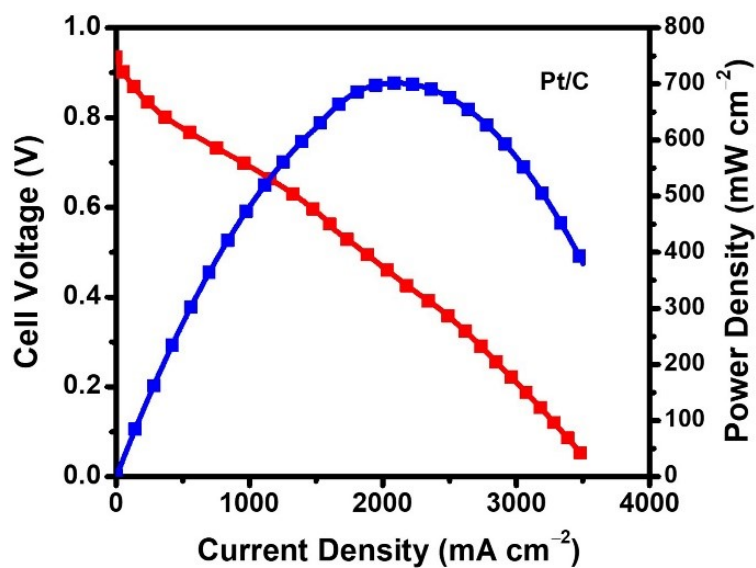


Fig. S13 AEMFC performance of Pt/C under 1.0 bar H_2/O_2 at 100 % relative humidity and 60 $^{\circ}\text{C}$.

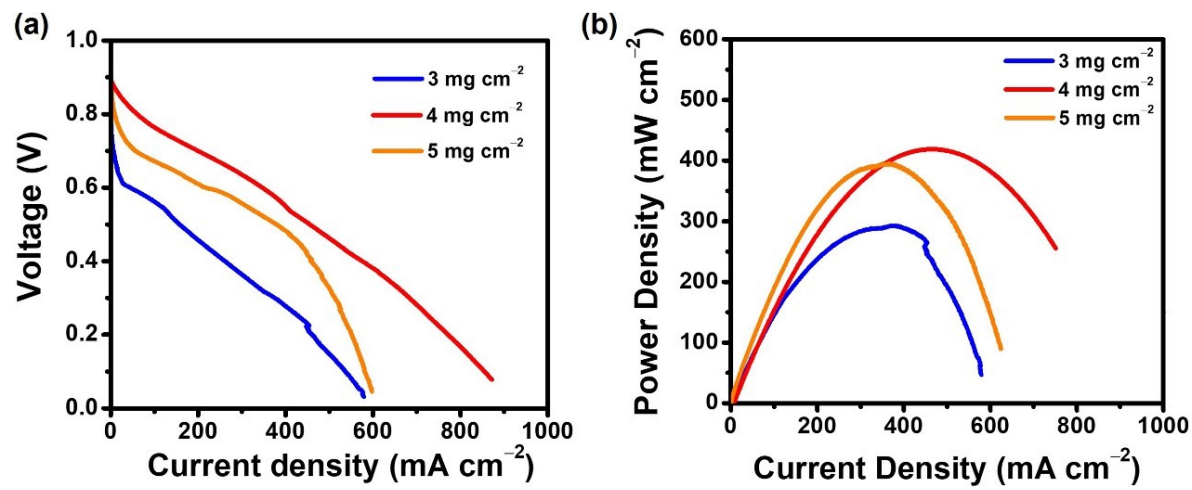


Fig. S14 (a, b) AEMFCs performances assembled with different loadings of Fe–N–C/GC under 1.0 bar H_2/O_2 at 100 % relative humidity and 60 °C.

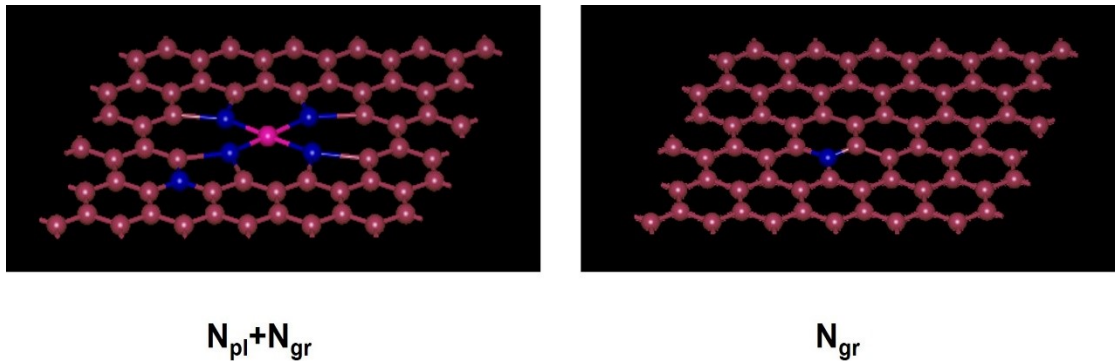


Fig. S15 Optimal DFT calculation models of $N_{pd}+N_{gr}$ and N_{gr} . Pink, blue, red represent Fe, N, C atoms, respectively.

Table S7. The calculated free energy of N_{pd} , N_{pl} , $N_{pd}+N_{gr}$, $N_{pl}+N_{gr}$ and N_{gr} intermediates.

Free energy (eV)	Clean surface	OH*	O*	OOH*
N_{pd}	-12046.495	-12511.210	-12480.913	-12942.770
N_{pl}	-11728.486	-12194.341	-12161.344	-12623.671
$N_{pd}+N_{gr}$	-12496.556	-12961.571	-12930.714	-13393.101
$N_{pl}+N_{gr}$	-11727.561	-12192.186	-12160.329	-12622.036
N_{gr}	-11476.704	-11940.329	-11911.672	-12372.179

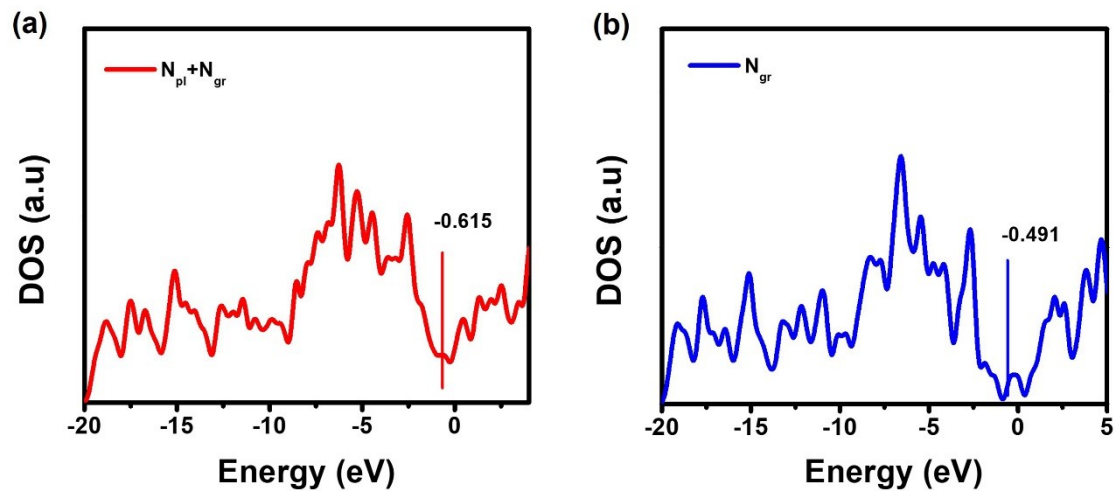


Fig. S16 Density of states on the $N_{pl} + N_{gr}$ and N_{gr} .

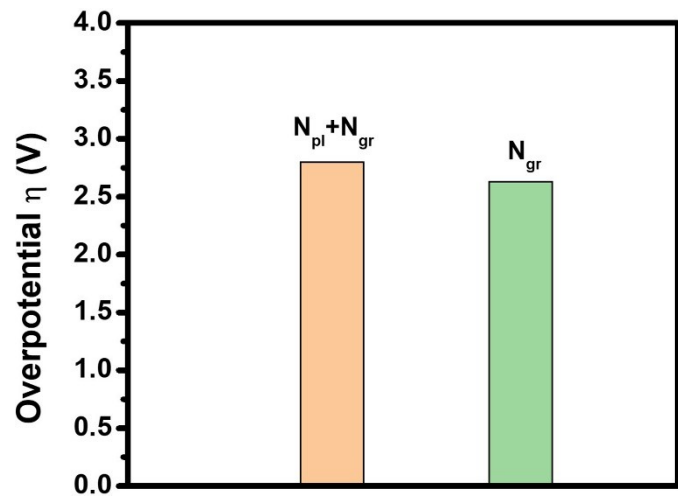


Fig. S17 The η values of ORR for the $N_{pl} + N_{gr}$ and N_{gr} .

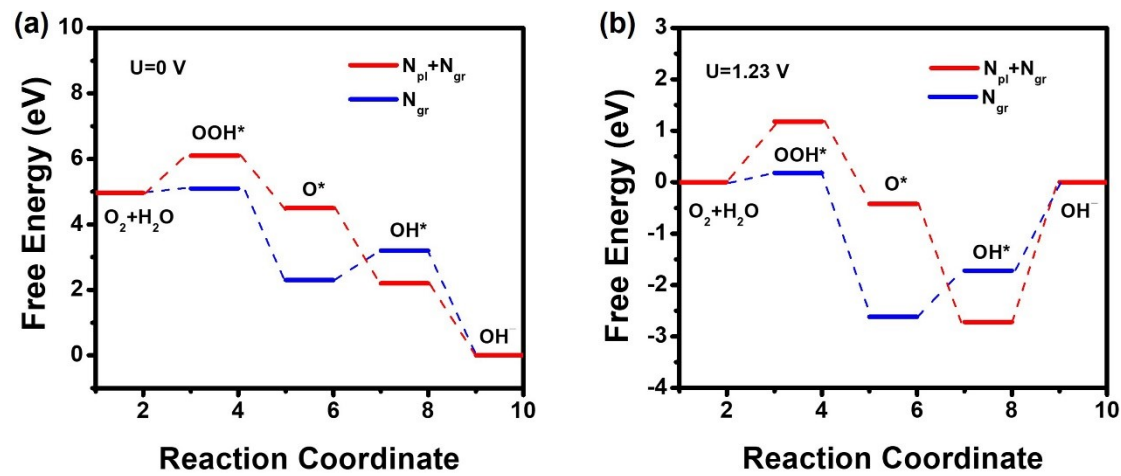


Fig. S18 Free energy diagram for ORR process on $\text{N}_{\text{pl}} + \text{N}_{\text{gr}}$ and N_{gr} models at the equilibrium potentials of $U=0 \text{ V}$ and $U=1.23 \text{ V}$.